

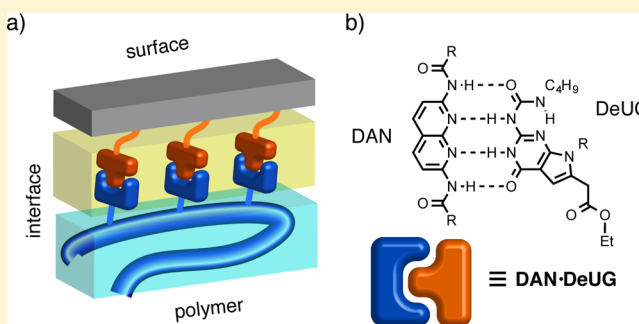
High-Affinity DNA Base Analogs as Supramolecular, Nanoscale Promoters of Macroscopic Adhesion

Cyrus A. Anderson,[†] Amanda R. Jones,^{‡,§} Ellen M. Briggs,[†] Eric J. Novitsky,[†] Darrell W. Kuykendall,[†] Nancy R. Sottos,^{‡,§,||} and Steven C. Zimmerman^{*,†}

[†]Department of Chemistry, [‡]Department of Mechanical Science and Engineering, [§]Beckman Institute for Advanced Science and Technology, and ^{||}Department of Materials Science and Engineering, University of Illinois at Urbana–Champaign, Urbana, Illinois 61801, United States

Supporting Information

ABSTRACT: Adhesion phenomena are essential to many biological processes and to synthetic adhesives and manufactured coatings and composites. Supramolecular interactions are often implicated in various adhesion mechanisms. Recently, supramolecular building blocks, such as synthetic DNA base-pair mimics, have drawn attention in the context of molecular recognition, self-assembly, and supramolecular polymers. These reversible, hydrogen-bonding interactions have been studied extensively for their adhesive capabilities at the nano- and microscale, however, much less is known about their utility for practical adhesion in macroscopic systems. Herein, we report the preparation and evaluation of supramolecular coupling agents based on high-affinity, high-fidelity quadruple hydrogen-bonding units (e.g., DAN·DeUG, $K_{\text{assoc}} = 10^8 \text{ M}^{-1}$ in chloroform). Macroscopic adhesion between polystyrene films and glass surfaces modified with 2,7-diamidonaphthyridine (DAN) and ureido-7-deazaguanine (DeUG) units was evaluated by mechanical testing. Structure–property relationships indicate that the designed supramolecular interaction at the nanoscale plays a key role in the observed macroscopic adhesive response. Experiments probing reversible adhesion or self-healing properties of bulk samples indicate that significant recovery of initial strength can be realized after failure but that the designed noncovalent interaction does not lead to healing during the process of adhesion loss.



INTRODUCTION

Adhesion is pervasive in nature and therefore found on length scales that range from small peptides to cells and whole organisms.¹ Man-made adhesives were first developed at least 5000 years ago.² Today adhesion phenomena are of central importance in commercial adhesives, coatings, and polymer composites.^{3,4} Poor interfacial properties can cause such systems to exhibit diminished mechanical performance or reduced surface protection. At the extreme, separation of the adhesive or coating from the substrate can cause failure of the material bond or full exposure of a protected surface. Although a number of explanations for the behavior of systems exhibiting good interfacial properties have been put forward, including effective wetting, mechanical interlocking, adsorption, and diffusion of resins, and electrostatic interactions, each is insufficient to explain fully or predict the performance of an adhesive bond.³ One common theme among adhesion theories, however, is that covalent and noncovalent interactions can improve the interfacial properties of a given system.³ A number of adhesion promoters or coupling agents have been successfully designed on these principles and often feature multifunctional compounds that bridge the interface between

adhesive and adherend.^{3b} Thus, there is an excellent link between supramolecular chemistry and adhesion science.

In recent years, synthetic DNA base-pair mimics have been pursued in the context of hydrogen-bond-mediated molecular recognition, self-assembly, and supramolecular polymer chemistry.⁵ Nucleobase mimics have also been used to probe adhesion phenomena. Thus, reversible and selective adsorption of polymer films and spatial control over the self-assembly of nanoparticles on surfaces have been achieved using specific hydrogen-bonding interactions.⁶ In other work, atomic force microscopy (AFM) force data suggest that complementary oligonucleotides and artificial nucleobases form noncovalent bonds across interfaces.⁷ Finally, hydrogen-bonded base-pair analogs have been used to stabilize incompatible polymer phases.⁸ Although covalent bonds and noncovalent interactions are widely used to improve interfacial adhesion, the use of specific hydrogen-bonding interactions, like those found among nucleobase mimics, has received little attention in macroscopic systems. This class of noncovalent interactions is particularly interesting for study in materials chemistry applications because

Received: January 24, 2013

it is intermediate in strength, with free energies of formation in apolar solvent (chloroform) that are 5–15% that of a C–C covalent bond. Thus, it is fully reversible and can often be highly selective. Use of these dynamic chemical bonds can enable self-healing and other smart materials systems.⁹

With the above considerations in mind, we reasoned that incorporating such complementary units onto surfaces and into polymeric adhesives might both improve the interfacial properties of disparate materials and realize useful properties, such as selective and reversible adhesion. Herein, we report the preparation and evaluation of a supramolecular adhesive system capable of forming a stable hydrogen-bonded complex across the interface between glass and a thermoplastic resin. Mechanical tests were used to quantify practical adhesion in bulk samples and elucidate the role of the supramolecular interactions.

RESULTS AND DISCUSSION

To determine whether the use of artificial nucleobase pairing can improve interfacial adhesion, we prepared and evaluated an adhesive and a glass surface (the adherend) each tailored with various DNA base-pair mimics such that the designed hydrogen-bonded complex could form across the interface (Figure 1a). The complementary DNA base-pair mimics 2,7-

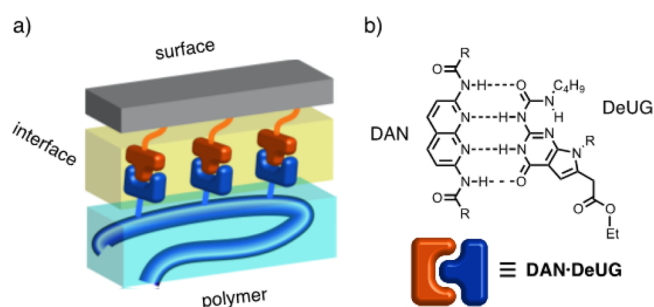


Figure 1. (a) Supramolecular coupling agents for improved interfacial adhesion. (b) The DNA base-pair mimics DAN and DeUG. The DAN·DeUG complex serves as the reversible noncovalent bond between the adhesive and the adherend.

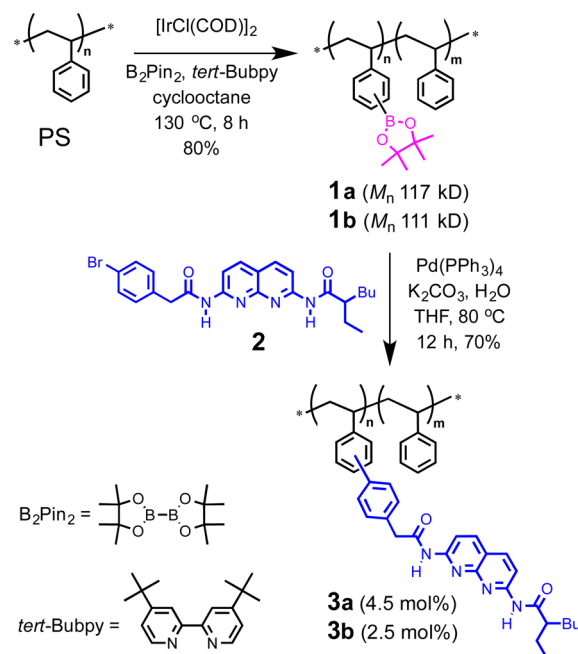
diamidonaphthyridine (DAN)¹⁰ and ureido-7-deazaguanine (DeUG)¹¹ were chosen for use in this work because the pair forms a very stable complex (Figure 1b, $K_{\text{assoc}} = 10^8 \text{ M}^{-1}$ in chloroform) and both the DeUG and DAN units self-associate minimally. Such binding properties make these units highly selective for the formation of the desired DeUG·DAN interaction. Furthermore, both units can be readily prepared with synthetic handles, allowing their incorporation into resins and onto surfaces.¹²

Polystyrene (PS) was selected for use as the adhesive because it is a glassy polymer at ambient temperature (i.e., $T_g > 100^\circ\text{C}$). This property means that viscoelastic flow is absent so that mechanical tests, e.g., by measuring shear strengths (*vide infra*), might better represent the interfacial effect of the supramolecular interactions.¹³ Furthermore, PS lacks polar functional groups that would otherwise participate in nonspecific hydrogen bonding with the nucleobase mimics present in this system.

Previously we prepared DAN-containing PS by copolymerization of styrene and a DAN functionalized styrene monomer.^{8a,b,e,12} Here an attractive alternative was pursued involving the C–H functionalization of commercially available

PS. Thus, multivalent PS graft copolymers featuring the DAN recognition unit were synthesized by analogy to the methods reported by Bae (Scheme 1).¹⁴ Thus, the C–H borylation of

Scheme 1



PS at 85 and 130°C gave polyboronic esters **1a** and **1b** in yields of 76% and 80%, respectively. The borylation attempt carried out at the lower temperature more typically gave yields closer to 50%, but the yields were closer to 80% when the reaction temperature was between 120 and 150°C . The number average molecular weights (M_n) and polydispersity index values (PDI) of the polymers are shown in Table 1.¹⁵

Table 1. Polymer M_n and PDI Values^a

polymer	M_n (kDa)	mol % DAN UV–vis (NMR)	PDI
PS	75	—	3.1
1a	117	—	2.5
3a	235	4.5 (5)	2.5
PS	69	—	2.0
1b	111	—	1.3
3b	114	2.5 (2)	1.3

^aDetermined by analytical SEC in DMF using PS standards. See Supporting Information for full details.

Subsequent Suzuki–Miyaura cross coupling of **1a,b** with aryl bromide **2**^{10e} gave DAN-functionalized PS **3a,b** in 35–65% overall recovery. Several points should be made about the synthesis of **3a,b**. First, the polymers were purified by precipitation so the decrease in PDI is a result of molecular weight fractionation. The increase in M_n may not only result from polymer fractionation but also likely reflects the DAN units inducing aggregation or a larger hydrodynamic radius, leading to a higher apparent PS-calibrated molecular weight. The amount of residual boronic acid was examined in two ways. The ^{11}B NMR spectrum of **1** showed a signal consistent with the aryl boronic ester, but no signal was observed in **3**. The low sensitivity of ^{11}B NMR meant that this method was not conclusive. The ICP-MS indicated some residual boron was

present in polymer 3, although it could not distinguish unreacted aryl boronic acid groups from residual boron-based byproducts of the Suzuki–Miyaura reaction. In either event, control experiments with boronic ester polymer 1 suggest little added adhesion relative to PS.

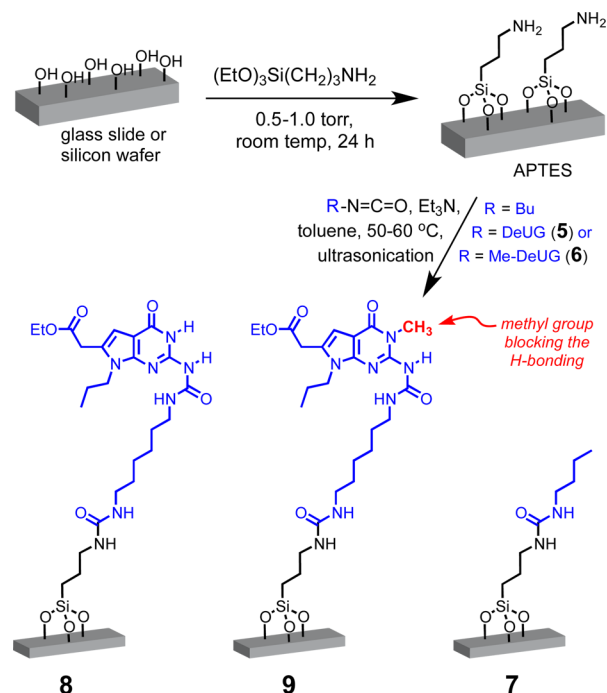
Both UV–vis and ^1H NMR were used to measure the incorporation of DAN into 3, both methods agreeing closely on the extent of the recognition unit loading. Beyond measuring the extent of incorporation, the UV–vis and ^1H NMR spectra are consistent with the DAN unit being linked to the polymer without alteration. Furthermore, ^1H NMR analysis of a CDCl_3 solution containing 3a and DeUG (see Figure 1) provides qualitative evidence that 3a is capable of forming DeUG–DAN complexes along its backbone. Thus, the pronounced downfield shift (2–4 ppm) of both the DAN and DeUG NH resonances upon mixing (Figure S1) indicates hydrogen-bond pairing. These data and its T_g of 135 $^\circ\text{C}^{15}$ indicate that 3a is a glass at ambient temperature and a complementary binder of the DeUG unit.

With the functionalized PS polymers prepared, attention was turned to the preparation of functionalized surfaces to which they might bond via base pairing. We chose to examine two scenarios that represent common practical applications for adhesives. The first involves the PS bonding of two glass or silicon surfaces bearing complementary DeUG units. The second study models fiberglass composite applications, looking at the direct interaction between the PS and the surface functionalized glass fibers. Despite having poor interfacial properties with many resins, glass fibers are widely used in fiber-reinforced composites.¹⁶ A number of reactive organo-silanes have been developed^{13b,17} to alleviate this problem, and many solution- and vapor-phase methods for the deposition of silanes have been devised.¹⁸

The functionalization of all surfaces started with the vapor-phase deposition of (3-aminopropyl)triethoxysilane (APTES). The vapor deposition method was used because it is known to produce uniform films,¹⁹ and the APTES surface could be treated with various functional isocyanates. Thus, glass microscope slides and oxidized silicon wafers bearing the DeUG and other recognition units were prepared accordingly as outlined in Scheme 2.¹⁵ Substrates were carefully cleaned and exposed to APTES vapor. In the case of glass and silicon wafers a schematic representation of the APTES surface is shown in Scheme 2. Although this is an idealized structure, the actual coating is likely polymeric (*vide infra*).¹⁹ The resulting amine-tailored APTES surfaces were treated with a solution of butylisocyanate, DeUG-isocyanate 5, or methylated DeUG (MeDeUG) isocyanate 6 to give the corresponding butyl (7), DeUG (8), and MeDeUG (9) surfaces, in each case the organic group linked to the surface through a urea linkage.

The physical properties of the functionalized surfaces were determined using water contact goniometry, ellipsometry, and AFM. Contact angles for surfaces 7–9 ranged from 55–70 $^\circ$, indicating that the functionalized surfaces are more hydrophobic than bare glass (water contact angle <10 $^\circ$), as is expected (Table S1). Ellipsometry of 7–9 on oxidized wafers indicated that these films had thicknesses of 3–4 nm. A CPK model of an extended APTES unit suggests that the thickness of a uniform monolayer is on the order of 0.5 nm, therefore, it is likely that these samples are polymeric films. Film quality was evaluated at the nanoscale by AFM. Surfaces appeared to be uniformly coated. Tapping-mode images for 3 \times 3 μm regions of each surface appear in Figure S2, and these data were used to

Scheme 2



measure the root-mean-squared (RMS) roughness for each surface (see Table S1). The untreated oxidized silicon wafer substrate and the resultant APTES films are relatively smooth, having a roughness <0.2 nm. Although the treatment of APTES films with the isocyanates did increase the roughness of the films, all surfaces have an RMS roughness <1 nm. The measured RMS roughness is smaller than the film thickness, suggesting that the films have uniform mass coverage.

The chemical nature of the films was examined using secondary ion mass spectrometry (TOF-SIMS), X-ray photoelectron spectroscopy (XPS), and UV–vis spectroscopy. Analysis of glass slides by TOF-SIMS revealed an increase in counts for organic fragments upon functionalization with APTES and butylisocyanate, as evident from the detection of fragments at or above 55 m/z (Figure S3).²⁰ Most importantly, analysis of surface 8 revealed a mass peak of significant intensity at 205 m/z , which is consistent with fragmentation of the DeUG heterocycle.¹⁵ In particular, this fragment, which cannot be detected on surfaces 7 and 9, is consistent with the deazaguanine unit core, having lost the carboxyethyl and urea linker groups.

XPS analysis of the bare substrate (oxidized silicon wafers), films of APTES, and 7–9 indicated that C and N content increased upon surface modification (Table S2). Although the observed C/N ratios are higher than expected, this finding can be attributed to unavoidable contamination with hydrocarbons during handling and storage. High-resolution C 1s and N 1s XPS data were collected for each sample and appear in Figure S4. The N 1s region of the APTES film indicates photoelectrons with binding energies that are consistent with amine and ammonium chemical bonding environments. The C 1s region for the APTES films indicates photoelectrons with binding energies that are consistent with saturated and heteroatom C environments. Overall, these data agree with previous analyses of APTES films on glass substrates.^{19b,21}

Functionalization of the APTES film with DeUG (surface 8) leads to significant changes in the high-resolution XPS data.

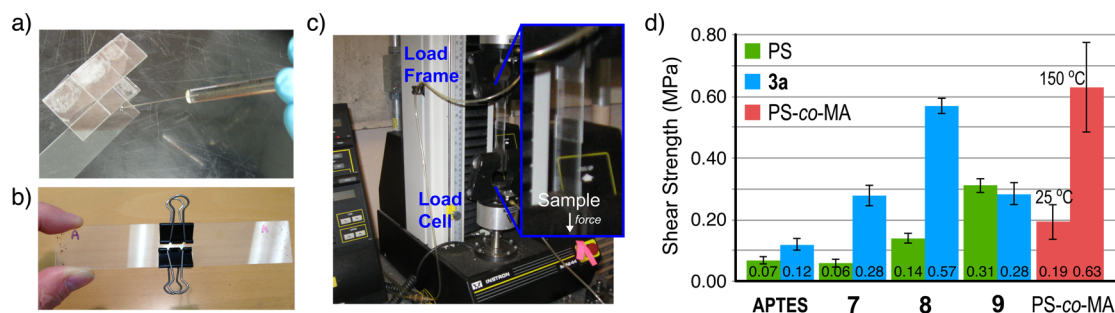


Figure 2. Lap-shear testing of virgin samples set with PS, DAN-functionalized PS **3a**, or PS-co-MA. (a) Samples ($n \geq 10$) were set with 10 μL of a 10 mg mL^{-1} solution of either **3a**, PS, or poly(styrene-co-maleic anhydride) (PS-co-MA) in CH_2Cl_2 . (b) The 15×25 mm overlaps were clamped in place and cured under ambient conditions for 72 h. Samples set with PS-co-MA were either cured under ambient conditions or were first cured under ambient conditions for 12 h and subsequently cured at 150°C for 12 h, followed by gradual cooling to ambient temperature. (c) All samples were sheared at 1 mm min^{-1} under ambient conditions. (d) Lap-shear test results: the mean shear strength is given, and error represents the standard error of the mean. The statistical significance of differences between mean shear strength values for PS and **3a** on surfaces APTES and 7–9 were calculated as p -values = 0.029 ($n = 10$), 0.0027 ($n = 4, 11$), <0.0001 ($n = 11, 12$), and 0.43 ($n = 5$), respectively.

The N 1s region broadens, and peak-fitting reveals photoelectron peaks that are consistent with urea and pyridone environments.²² Similarly, the C 1s region broadens, and peak-fitting is consistent with saturated, heteroatom, and carbonyl C environments.²³ XPS data for APTES films treated with butylisocyanate (surface 7) were collected to examine the contribution of the urea moiety linking each recognition unit to the surface. Photoelectron peaks in the N 1s and C 1s region are consistent with urea–N environments as well as saturated and carbonyl C environments. The XPS data for surfaces 8 and 9 are quite similar to each other, consistent with the nearly identical chemical structures of their added layers. Further, they both contain elements seen in 7 indicating the presence of the linker group, yet both had additional intensities consistent with their treatment with isocyanates 5 and 6. Overall, these data are consistent with the covalent surface functionalization shown in Scheme 2.

As a final test to see whether the functionalization process might alter the integrity of the recognition unit, the chemistry was applied to quartz slides enabling surface characterization by UV–vis spectroscopy. To use a second chromophore with a different spectrum for comparison, a DAN isocyanate was prepared and reacted with the quartz slide alongside DeUG isocyanate **5**.¹⁵ Analysis of the films was accomplished by placing the modified substrates in the optical path of the spectrometer,²⁴ with the recorded spectra shown in Figure S5. APTES films are featureless with no appreciable absorbance from 250–400 nm. Surfaces treated with the DAN- and DeUG-isocyanates produced spectra similar to that of DAN and DeUG derivatives in solution. These measurements confirm that the recognition unit remains intact throughout the functionalization process. Further, repeated washing of the modified substrates did not cause a change in the measured absorbance intensity supporting covalent surface attachment.

Lap-shear tests were performed to evaluate the adhesive properties of the supramolecular coupling agents.³ Samples were prepared by injecting a small volume of a methylene chloride (CH_2Cl_2) solution of **3a** or unmodified PS onto microscope slides bearing films of APTES or 7–9 (Figure 2a). Slides were mated, clamped in place, and cured under ambient conditions (Figure 2b). The resultant samples were sheared at 1 mm min^{-1} until failure (Figure 2c). As seen in Figure 2d, samples of APTES, 7, and 8 set with PS gave comparatively low shear strengths in the range of 0.06–0.14 MPa. Likewise, DAN-

functionalized PS **3a** exhibited poor adhesion to the APTES layer (0.12 MPa) but a stronger interaction with the butyl urea coated surface 7 (0.28 MPa). The latter case indicates that the urea linkage is likely to contribute when dipolar- or hydrogen-bonding interactions to the resin are possible. As indicated above, residual boron was detected in polymer **3**, and a further nonspecific contribution from a small amount of residual arylboronic acid cannot be ruled out, however, the adhesive properties of **1** were examined and found to be poor.

Use of DAN polymer **3a** with DeUG surface 8 introduces the possibility of specific hydrogen-bonding interactions between DAN in the polymer and DeUG on the surface. Indeed, samples of 8 set with **3a** gave a shear strength of 0.57 MPa, which is higher than any other pairing examined and significantly greater than control experiments performed with unmodified PS.

Strong supporting evidence for the participation of the designed quadruply hydrogen-bonded DeUG–DAN pairing in the adhesive response was obtained by comparing DeUG surface 8 to MeDeUG surface 9 (Figure 2d). These two surfaces are identical except for a single methyl group on the N1-position of the deazaguanine unit of 9. In chloroform solution, single methylation decreases the association constant (K_{assoc}) by at least 6 orders of magnitude. Indeed, ^1H NMR binding studies in chloroform- d indicated that the MeDeUG–DAN complex has a $K_{\text{assoc}} < 100 \text{ M}^{-1}$ (Figure S6), whereas that for the analogous DeUG–DAN complex was measured by isothermal titration calorimetry (ITC) to be $K_{\text{assoc}} \approx 2 \times 10^8 \text{ M}^{-1}$ in chloroform.^{11b} Samples of 9 set with either PS or **3a** gave similar shear strengths of ~ 0.30 MPa. Although these surfaces have similar physical properties (Table S1), the shear strength measured for samples of **3a** on 9 is significantly less than that measured for samples of **3a** on 8. Furthermore, the shear strength measured for **3a** on 9 is in line with shear strengths measured for **3a** on 7, which suggests that the urea, rather than the blocked DNA mimic, primarily contributes to the strength of the adhesion.

What is the origin of the differing adhesive strengths seen in Figure 2d? Macroscopic measurements of the surface properties do not correlate with the adhesive strengths observed. For example, each surface wets to a similar extent when in contact with the polymer solution (Table S3). Furthermore, there is no clear relationship between surface energy (Table S1) and bond strength, as observed by others,²⁵ suggesting that origin of the

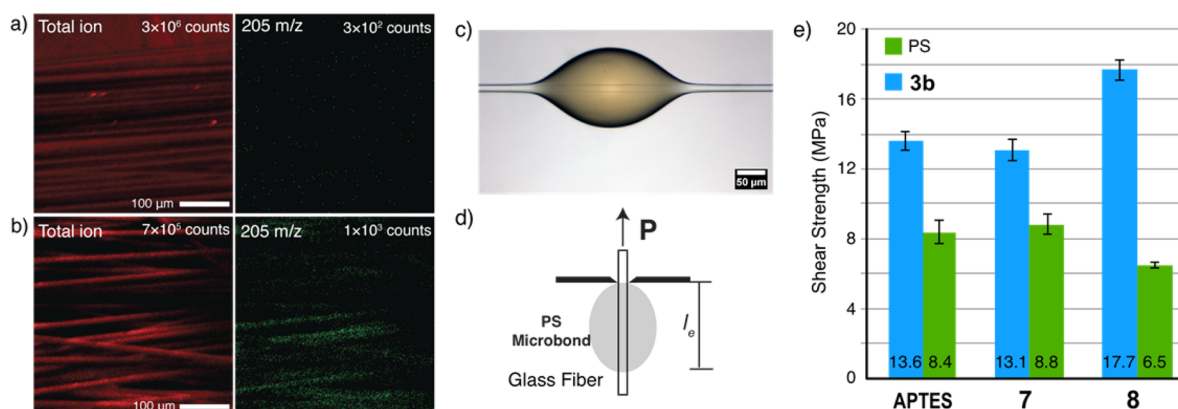


Figure 3. (a) TOF-SIMS analysis of E-glass fibers (a) as received and (b) upon treatment with DeUG isocyanate 5. Mass spectral peak at $m/z = 205$ corresponds to molecular fragment diagnostic of the DeUG heterocycle. (c) Single-fiber pull test specimen used a bead of 3b on a DeUG-treated fiber 8. (d) Schematic of apparatus used for single-fiber-pull tests. (e) Interfacial shear strength determined for beads of 3b and PS on fibers having the APTES, 7, and 8 surface treatments. Mean shear strengths are given, and error represents standard error of the mean. The statistical significance of differences between mean shear strength values for PS and 3b embedded with fibers coated with APTES, 7, and 8 were calculated as p -values = <0.0001 ($n = 11, 27$), 0.0002 ($n = 8, 14$), and <0.0001 ($n = 20, 35$), respectively.

behavior of this system lies at the nano- and microscale. A qualitative, visual inspection indicated that samples set with 3a underwent primarily cohesive failure, whereas samples set with PS underwent mixed adhesive–cohesive failure. This behavior is consistent with improved interfacial properties for the designed DeUG–DAN base-pairing system. However, further experiments probing the chemical and morphological properties at the nano- and microscale are necessary to elucidate the full details of the failure mode.

The above observations do support a connection between the supramolecular interaction and the observed adhesive properties. Adhesion resulting directly from hydrogen-bonding interactions is certainly possible. Other explanations for the observed trend in shear strength could be that base-pairing mediated self-assembly promotes either the formation of a tightly bound film of 3a or the diffusion of 3a into the silane layer, thereby improving the strength of the interface relative to samples set with unmodified PS.

Comparisons with traditional adhesives are difficult to make given the many experimental variables involved. However, the performance of the supramolecular adhesive was compared to a conventional adhesion promoter, PS-*co*-maleic anhydride (Figure 2d).²⁶ Poly(styrene-*co*-maleic anhydride) (PS-*co*-MA) features anhydride moieties along the polymer backbone and is capable of covalent bonding with the APTES coating through imide formation. Lap-shear samples pairing the APTES surface with PS-*co*-MA were prepared and cured under the same conditions as used with the supramolecular agents above. An additional set was prepared and cured under nitrogen at 150 °C for 12 h, conditions used for various adhesive and composite formulations where PS-*co*-MA is used as an adhesion promoter.²⁷

Samples prepared with PS-*co*-MA and cured at ambient conditions indicated a shear strength of 0.19 MPa, whereas samples cured at 150 °C had measured shear strengths of 0.63 MPa. Therefore, in the case of PS-*co*-MA cured at ambient temperature, there is no improvement in shear strength relative to PS. Samples cured at the elevated temperature showed significantly improved shear strength. Interestingly, this improvement and the overall strength were within experimental error of the supramolecular system (DeUG surface 8 with 3a and cured at ambient temperature). Thus, one advantage of the

supramolecular system in this particular comparison is enabling strong bonding of two materials under mild conditions.

As noted above, glass fiber-reinforced composites are widely used in many different applications even though the glass has poor interfacial properties with many resins. To test whether this interface could be stabilized by the DeUG–DAN supramolecular interaction, single-fiber pull tests were developed to evaluate the performance of such composites. To this end, E-glass fibers were prepared displaying the DeUG unit.¹⁵ Support for the presence of the DeUG unit was obtained by TOF-SIMS analysis. As seen in Figure 3a,b, there was a significantly higher level of overall ion counts as well as a higher level of counts at $m/z = 205$; this mass corresponding to the DeUG unit.

Single fibers were embedded into a matrix of either PS or 3b (Figure 3c) as previously described.²⁸ Upon curing, the samples were loaded to failure as shown schematically in Figure 3d; test results appear in Figure 3e. As with lap-shear tests, samples set with PS gave lower interfacial shear strengths (IFSS) than samples set with the DAN-functionalized polymer. Although fibers featuring APTES and butylurea surfaces gave similar shear strengths when set with 3b, DeUG fibers gave the highest shear strength. The IFSS for the 3b–DeUG bond is comparable to glass fiber–epoxy bonds (~20 MPa).²⁹ Interestingly, the use of DAN–PS with only 2.5 mol % loading of the recognition unit was capable of producing an improved adhesive strength.

To explore the self-mending properties of this supramolecular-assisted adhesive, failed lap-shear samples of the DeUG surface 8, initially set with PS and PS–DAN 3a (Figure 2), were subjected to additional set–cure–test cycles. Thus, samples that were set with PS and sheared showed an average initially measured shear strength of 0.17 ± 0.02 MPa (Figure 4a), a value similar to what was seen in Figure 2 for a weak, nonspecific bond. The failed samples were then reset with 10 μ L of CH₂Cl₂ only, cured, and retested. The measured shear strength of the reset sample was 0.11 ± 0.03 MPa, a slight decrease that was just outside of experimental error. When samples set with 3a were subjected to this cycle, the first reset exhibited the enhanced adhesion seen in the DeUG–DAN pairings, although only 55% recovery of virgin shear strength was observed. The samples could be failed and reset two additional times before the shear strength decreased to a level

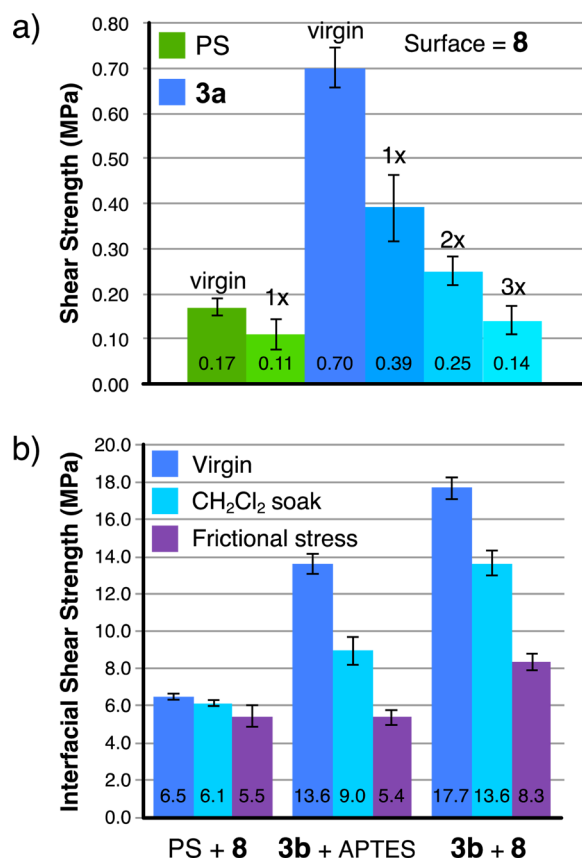


Figure 4. (a) Lap-shear testing of sheared samples reset with CH₂Cl₂ and cured under ambient conditions. Samples were first set with either 3a or PS and cured and failed as above. Failed samples were then reset with only 10 μ L of CH₂Cl₂ and cured and failed as above. This process was repeated several times. The mean shear strength is given, and error represents the standard error of the mean. (b) Single-fiber pull tests assessing recovery of initial shear strength upon immersion in CH₂Cl₂. The frictional force measured from dragging the polymer bead along the fiber is included for reference.

comparable to that of samples set with unmodified polymer. These data are attributed to an inability of the base-pair mimics to reform the specific complex; this in turn could be due to contamination or damage of the interface upon failure.

To minimize contamination of the interface and crack separation, the single-fiber pull tests were also subjected to reset testing. Thus, virgin samples were prepared, loaded to failure, and then immersed in CH₂Cl₂. Upon drying, these samples were loaded to failure; data for the virgin and repaired samples are shown in Figure 4b. As was seen before (Figure 3e), the matched case of DAN–PS 3b on DeUG-modified fibers gives the highest interfacial shear strength, whereas control systems lacking either DAN or DeUG at the interface afforded lower shear strengths. The reset of the 3b DeUG-modified fiber system gave 77% recovery, ~20% improvement over lap-shear testing while using only half the mol % loading of recognition unit. In comparison, the 3b APTES-modified fiber system gave 66% recovery. Relative to the APTES modified fibers, those displaying DeUG units gave stronger initial adhesion, but only a very small additional benefit from the hydrogen-bonding pair was seen in the recovery cycle. In Figure 4b, the inherent frictional stresses generated during the fiber pull-out process are also compared to both the virgin IFSSs and the reset values. An IFSS that is close to the frictional stress indicates minimal

chemical bonding. In the case of PS bonded with 8, the recovery was within error of the friction between the two interfaces.

SUMMARY AND CONCLUSIONS

We previously reported the DeUG–DAN supramolecular system as a type of enhanced DNA base pair, showing significantly higher stability and affinity than AT and GC. Herein we applied this quadruply hydrogen-bonded pair as supramolecular coupling agents that can function as nanoscale adhesive agents for improving interfacial interactions. Commercially available PS was functionalized with the DAN unit using a C–H activation methodology, and glass surfaces were treated with complementary DeUG. Two applications were examined, one in which the polymer served as an adhesive bonding two glass surfaces together, and the other modeling glass fiber-reinforced composites.

Mechanical test data in both situations are consistent with the DAN–DeUG interaction playing a role in the adhesive response. Indeed, bonds of comparable strength to those formed using conventional adhesion promoters that utilize covalent bonds were observed. In the case of the single glass fiber microbond specimens, only 2.5 mol % recognition units were required to demonstrate this improved adhesion. Advantages of the supramolecular system are the lower temperatures under which the adhesive could be set and the ability to reset adhesive joints without adding additional material, only solvent. Although not studied here one can easily envision stimuli-responsive behavior when using hydrogen-bonding units that can be turned on and off reversibly.^{8c}

Self-healing potential was explored for both lap-shear and single fiber experiments. In the lap-shear experiments, up to 55% recovery was demonstrated, and three resets were possible before the shear strength was reduced to the level of unmodified polymer. For single fiber tests, up to 77% recovery was demonstrated using just over half the recognition unit. Additional studies are needed to better understand the role of the nanoscale adhesive agents in increasing the interfacial interaction. It was also observed that the urea linkage used to connect the recognition units to the surfaces led to a significant nonspecific adhesive interaction. Studies are ongoing to explore alternative methods of coating the surfaces that would enhance the role played by the hydrogen-bonding units. One ultimate goal would be extremely strong adhesives that could be readily reversed upon addition of a competitive solvent or by a stimuli responsive recognition unit.

METHODS

Polymer Modification. C–H borylation of PS using B₂Pin₂ in the presence of [IrCl(COD)]₂ and *tert*-Bubpy in cyclooctane or THF, according to the method of Bae¹⁴ gave polyboronic ester 1a–b. Subsequent Suzuki–Miyaura cross coupling of 1a,b with aryl bromide 2 using Pd(PPh₃)₄ and K₂CO₃ in THF/H₂O, by analogy to Bae¹⁴ gave DAN-functionalized PS 3a,b in 35–65% overall recovery.

Surface Modification. Glass microscope slides and oxidized silicon wafers were carefully cleaned using piranha solution, washed, dried, and exposed to APTES vapor at ambient temperature and 0.5–1 Torr for 24 h. The resulting surfaces were washed, dried, and treated with a solution of butylisocyanate, DeUG–isocyanate 5, or methylated DeUG (MeDeUG) isocyanate 6 in toluene in the presence of triethylamine under ultrasonication at 50–60 °C for 24 h. The resulting butylurea 7, DeUG 8, and MeDeUG 9 surfaces were finally washed, dried, and used for surface analysis or preparation of samples for mechanical testing. Glass fibers were washed with toluene and

gently stirred in a solution of DeUG isocyanate **5** and triethylamine in toluene as above. The resulting fibers were washed, dried, and used for analysis and mechanical tests.

■ ASSOCIATED CONTENT

● Supporting Information

Contact angles for surfaces 7–9. This material is available free of charge via the Internet at <http://pubs.acs.org>.

■ AUTHOR INFORMATION

Corresponding Author

sczimmer@illinois.edu

Notes

The authors declare no competing financial interest.

■ ACKNOWLEDGMENTS

S.C.Z. acknowledges support by the NSF (CHE-1012212). The work was carried out in part at the Frederick Seitz Materials Research Laboratory Central Facilities, University of Illinois, which is supported in part by the U.S. Department of Energy under grants DE-FG02-07-ER46453 and DE-FG02-ER46471. C.A.A. acknowledges the University of Illinois Department of Chemistry for an R. Carr graduate fellowship. Timothy Spila, Richard Haasch, and Scott MacLaren are thanked for assistance with surface analysis (TOF-SIMS, XPS, and AFM). A.R.J. and N.R.S. acknowledge the support of the Air Force Office of Scientific Research (FA9550-10-1-0126) and NSF (CMMI-1161517).

■ REFERENCES

- (1) (a) Dubiel, E. A.; Martin, Y.; Vermette, P. *Chem. Rev.* **2011**, *111*, 2900–2936. (b) *Biological Adhesives*; Smith, A. M., Callow, J. A., Eds.; Springer-Verlag: Berlin, 2006. (c) *Biological Adhesive Systems. From Nature to Technical and Medical Application*; von Byern, J., Grunwald, I., Eds.; Springer-Verlag: Wien, 2010.
- (2) See: Onusseit, H., ref 1c, Chapter 12.
- (3) (a) Pocius, A. V. *Adhesion and Adhesives Technology*, Hanser: Munich, 2002. (b) Petrie, E. M. *Handbook of Adhesives and Sealants*, McGraw-Hill: Chicago, 2007.
- (4) Wicks, Z. W.; Jones, F. N.; Pappas, P. S. & Wicks, D. A. *Organic Coatings: Science and Technology*, 3rd Ed., Wiley: Hoboken, 2007.
- (5) (a) Zimmerman, S. C.; Corbin, P. S. *Struct. Bonding (Berlin)* **2000**, *96*, 63–94. (b) Sivakova, S.; Rowan, S. J. *Chem. Soc. Rev.* **2005**, *34*, 9–21. (c) Binder, W. H.; Zirbs, R. *Adv. Polym. Sci.* **2007**, *207*, 1–78. (d) Wilson, A. J. *Soft Matter* **2007**, *3*, 409–425. (e) Gong, B. *Polym. Int.* **2007**, *56*, 436–443. (f) de Greef, T. F. A.; Smulders, M. M. J.; Wolfs, M.; Schenning, A. P. H. J.; Sijbesma, R. P.; Meijer, E. W. *Chem. Rev.* **2009**, *109*, 5687–5754. (g) Fathalla, M.; Lawrence, C. M.; Zhang, N.; Sessler, J. L.; Jayawickramarajah, J. *Chem. Soc. Rev.* **2009**, *38*, 1608–1620. (h) Yang, S. K.; Ambade, A. V.; Weck, M. *Chem. Soc. Rev.* **2011**, *40*, 129–137.
- (6) (a) Norsten, T. B.; Jeoung, E.; Thibault, R. J.; Rotello, V. M. *Langmuir* **2003**, *19*, 7089–7093. (b) Viswanathan, K.; Ozhalici, H.; Elkins, C. L.; Heisey, C.; Ward, T. C.; Long, T. E. *Langmuir* **2006**, *22*, 1099–1105. (c) Xu, H.; Hong, R.; Lu, T.; Uzun, O.; Rotello, V. M. *J. Am. Chem. Soc.* **2006**, *128*, 3162–3163. (d) See also: Harada, A.; Kobayashi, R.; Takashima, Y.; Hashidzume, A.; Yamaguchi, H. *Nat. Chem.* **2010**, *3*, 34–37.
- (7) (a) Kersey, F. R.; Lee, G.; Marszalek, P.; Craig, S. L. *J. Am. Chem. Soc.* **2004**, *126*, 3038–3039. (b) Zou, S.; Schönherr, H.; Vancso, G. J. *J. Am. Chem. Soc.* **2005**, *127*, 11230–11231.
- (8) (a) Park, T.; Zimmerman, S. C.; Nakashima, S. *J. Am. Chem. Soc.* **2005**, *127*, 6520–6521. (b) Park, T.; Zimmerman, S. C. *J. Am. Chem. Soc.* **2006**, *128*, 14236–14237. (c) Feldman, K. E.; Kade, M. J.; de Greef, T. F. A.; Meijer, E. W.; Kramer, E. J.; Hawker, C. J. *Macromolecules* **2008**, *41*, 4694–4700. (d) Kuo, S. W.; Cheng, R. S. *Polymer* **2009**, *50*, 177–188. (e) Li, Y.; Park, T.; Quansah, J. K.; Zimmerman, S. C. *J. Am. Chem. Soc.* **2011**, *133*, 17118–17121. (f) Wong, C.-H.; Zimmerman, S. C. *Chem. Commun.* **2013**, *49*, 1679–1695.
- (9) (a) Stuart, M. A. C.; Huck, W. T. S.; Genzer, J.; Müller, M.; Ober, C.; Stamm, M.; Sukhorukov, G. B.; Szleifer, I.; Tsukruk, V. V.; Urban, M.; Winnik, F.; Zauscher, S.; Luzinov, I.; Minko, S. *Nat. Mater.* **2010**, *9*, 101–113. (b) Murphy, E. B.; Wudl, F. *Prog. Polym. Sci.* **2010**, *35*, 223–251. (c) Blaszczak, B. J.; Kramer, S.; Olugebefola, S. C.; Moore, J. S.; Sottos, N. R.; White, S. R. *Ann. Rev. Mater. Res.* **2010**, *40*, 179–211. (d) Murphy, E. B.; Wudl, F. *Prog. Polym. Sci.* **2010**, *35*, 223–251. (e) Wojtecki, R. J.; Meador, M. A.; Rowan, S. J. *Nat. Mater.* **2011**, *10*, 14–27.
- (10) (a) Corbin, P.; Zimmerman, S. C. *J. Am. Chem. Soc.* **1998**, *120*, 9710–9711. (b) Corbin, P.; Zimmerman, S. C.; Thiessen, P. A.; Hawryluk, N. A.; Murray, T. J. *J. Am. Chem. Soc.* **2001**, *123*, 10475–10488. (c) Park, T.; Mayer, M. F.; Nakashima, S.; Zimmerman, S. C. *Synlett* **2005**, 1435–1436. (d) Mayer, M. F.; Nakashima, S.; Zimmerman, S. C. *Org. Lett.* **2005**, *7*, 3005–3008. (e) Lighthart, G. B. W. L.; Ohkawa, H.; Sijbesma, R. P.; Meijer, E. W. *J. Org. Chem.* **2006**, *71*, 375–378. (f) Anderson, C. A.; Taylor, P. G.; Zeller, M. A.; Zimmerman, S. C. *J. Org. Chem.* **2010**, *75*, 4848–4851.
- (11) (a) Ong, H. C.; Zimmerman, S. C. *Org. Lett.* **2006**, *8*, 1589–1592. (b) Kuykendall, D. W.; Anderson, C. A.; Zimmerman, S. C. *Org. Lett.* **2009**, *11*, 61–64.
- (12) (a) Park, T.; Zimmerman, S. C. *J. Am. Chem. Soc.* **2006**, *128*, 11582–11590. (b) Zhang, Y.; Zimmerman, S. C. *Beilstein J. Org. Chem.* **2012**, *8*, 486–495.
- (13) Ahagon, A.; Gent, A. N. *J. Polym. Sci., Polym. Phys. Ed.* **1975**, *13*, 1285–1300.
- (14) (a) Shin, J.; Jensen, S. M.; Ju, J.; Lee, S.; Xue, Z.; Noh, S. K.; Bae, C. *Macromolecules* **2007**, *40*, 8600–8608. (b) Jo, T. S.; Kim, S. H.; Shin, J.; Bae, C. *J. Am. Chem. Soc.* **2009**, *131*, 1656–1657.
- (15) See Supporting Information for full details of the characterization and experimental methods used in this study.
- (16) Jones, F. R. *J. Adhes. Sci. Technol.* **2010**, *24*, 171–202.
- (17) Matison, J. G. In *Silanes and Other Coupling Agents*; Mittal, K. L., Ed.; Brill: Leiden, 2009; Vol. 5, pp 3–23.
- (18) (a) Howarter, J. A.; Youngblood, J. P. *Langmuir* **2006**, *22*, 11142–11147. (b) Wang, W.; Vaughn, M. W. *Scanning* **2008**, *30*, 65–77. (c) Pasternack, R. M.; Amy, S. R.; Chabal, Y. J. *Langmuir* **2008**, *24*, 12963–12971. (d) Zhang, F.; Sautter, K.; Larsen, A. M.; Findley, D. A.; Davis, R. C.; Samha, H.; Linford, M. R. *Langmuir* **2010**, *26*, 14648–14654.
- (19) (a) Jung, G. Y.; Li, Z.; Wu, W.; Chen, Y.; Olynick, D. L.; Wang, S. Y.; Tong, W. M.; Williams, R. S. *Langmuir* **2005**, *21*, 1158–1161. (b) George, A.; Blank, D. H. A.; ten Elshof, J. E. *Langmuir* **2009**, *25*, 13298–13301. (c) Dorvel, B.; Reddy, B., Jr.; Block, I.; Mathias, P.; Clare, S. E.; Cunningham, B.; Bergstrom, D. E.; Bashir, R. *Adv. Funct. Mater.* **2010**, *20*, 87–95.
- (20) Wang, D.; Jones, F. R. *Surf. Interface Anal.* **1993**, *20*, 457–467.
- (21) Liu, X.; Thomason, J. L.; Jones, F. R. *J. Adhes.* **2008**, *84*, 322–338.
- (22) (a) Kelemen, S. R.; Gorbaty, M. L.; Kwiatek, P. J. *Energy Fuels* **1994**, *8*, 896–906. (b) Jansen, R. J. J.; van Bekkum, H. *Carbon* **1995**, *33*, 1021–1027.
- (23) (a) Shard, A. G.; Sartore, L.; Davies, M. C.; Ferruti, P.; Paul, A. J.; Beamson, G. *Macromolecules* **1995**, *28*, 8259–8271. (b) Perruchot, C.; Watts, J. F.; Lowe, C.; White, R. G.; Cumpson, P. J. *Surf. Interface Anal.* **2002**, *33*, 869–878.
- (24) Flink, S.; van Veggel, F. C. J. M.; Reinhoudt, D. N. *J. Phys. Org. Chem.* **2001**, *14*, 401–415.
- (25) (a) Levine, M.; Ilkka, G.; Weiss, P. J. *Polym. Sci., Part B: Polym. Lett.* **1964**, *2*, 915–919. (b) Barbarisi, M. J. *Nature* **1967**, *215*, 383–384.
- (26) (a) Triacca, V. J.; Ziaee, S.; Barlow, J. W.; Keskkula, H.; Paul, D. R. *Polymer* **1991**, *32*, 1401–1413. (b) Scholtens, B. J. R.; Brackman, J. C. *J. Adhes.* **1995**, *52*, 115–129.
- (27) Devaux, E.; Pak, S. H.; Cazé, C. *Polym. Test.* **2002**, *21*, 773–779.

- (28) Jones, A. R.; Blaiszik, B. J.; White, S. R.; Sottos, N. R. *Compos. Sci. Technol.* **2013**, 79, 1–7.
- (29) Blaiszik, B. J.; Baginska, M.; White, S. R.; Sottos, N. R. *Adv. Funct. Mater.* **2010**, 20, 3547–3554.